International Journal of
INTELLIGENT SYSTEMS AND APPLICATIONS IN ENGINEERING
ISSN:2147-6799 www.ijisae.org Original Research Paper

Non-Invasive Simulation Technique for Early Stroke Recognition Using Differentiation in Magnetic Flux Density Waves

Ahmed El-Shahat [1], Waleed. A [1],. Khaled S. Ahmed [1]

Submitted: 12/11/2022 **Revised:** 14/01/2023 **Accepted:** 11/02/2023

Abstract: Stroke is one of the most prevalent diseases around the world and identifying the type of stroke early is one of the most important reasons for effective treatment before the resulting death occurs or even before the complications of the disease occur and the permanent or semi-permanent disability it causes, and this is what many of those affected suffer from it by stroke. Therefore, early recognition of stroke is one of the preventative causes and one of the most important branches of scientific research in the medical field or medical engineering technology. The methods currently available for early identification of stroke, the most famous of which are computerized Tomography -CT scan and Magnetic Resonance Imaging -MRI scan, are not highly effective, despite the great development in these two methods used to detect stroke, they still have a significant shortcoming in early identification due to the delay in diagnosis, which causes a lot of death for patients or delays treatment, which leads to permanent disability, in addition to their lack of availability. In many hospitals because of their high prices, and for these reasons, the research point was chosen to overcome some of these current problems by developing a new model in which the artery was designed, the effect of electromagnetic waves was studied, and the change in Magnetic Flux Density through three designs of the artery, whether in its normal state, or in the event of an Ischemic stroke type where is the clotting of blood inside the artery, and the third case which is the hemorrhagic stroke where the artery cut, The results of the experiments in modeling the artery between the three cases were different in the value of the magnetic flux density waves, which contributes to setting a nucleus for the identification of stroke detection by electromagnetic waves, which can be developed in the future to be a good and fast solution at a cost much lower than the available techniques and this is the main goal of this research..

Keywords: *Artery Modeling, Changing the Magnetic Flux Density while Stroke, Electromagnetic waves in Brain, Stroke Simulation, Stroke Recognition.*

1. Introduction

Stroke is one of the most important areas of research that needs a lot of effort, as it is related to one of the most dangerous diseases for patients, and ischemic stroke, which is the occurrence of intra-artery clotting or the hemorrhagic, which is the occurrence of intra-artery cutting [1,2]. In both cases, if the brain cells are affected by clotting or bleeding, these dead cells that have been affected will not work again, and this is the main reason for deaths with several more than six million annually or living with a permanent disability if the discovery is delayed by 70% of patients who have been diagnosed. Late discovery of their condition. The research aimed to find a new and innovative way to identify both types of strokes through the change in the rays of electromagnetic waves, especially the change in the waves of Magnetic Flux Density, This method that was relied on in this research paper is fast, less expensive and very effective in identifying the type of stroke, which is necessary to prevent deaths due to this disease or reduce the impact of complications resulting from delaying the detection of this stroke, whether using CT [3,4]. or MRI [5,6]., where the methodology of this research paper is based on studying the change in the effect of Magnetic Flux Density through different designs of the artery in the normal, Ischemic or Hemorrhagic case, where the Magnetic Flux Density is studied through a perpendicular region, which represents the number the total magnetic field lines that pass through this region by the magnetic flux formula μ which is the permeability of the medium or material in which the fields are measured. Multi-Physics simulations have been used between the geometry of our designed model that represents normal artery blood flow, clotting, or cutting to determine the early detection of stroke non-invasively [7-10], where this technique does not require intervention. in the way that is done in the current techniques such as available imaging devices, it only requires directing electromagnetic waves near the artery and then, measuring the extent of the change in the Magnetic Flux Density according to each type through the model designed for the artery [11-14]. and this depends largely on the management of the disease initiation from early detection according to symptoms, lower cost, and high speed.

1 Ahmed El-Shahat. Faculty of Engineering, Benha University,– 16811, Egypt
ORCID ID : 0000-0003-4716-1023
1 Khaled S Ahmed. Faculty of Engineering, Benha University,– 16811, Egypt
ORCID ID : 0000-0002-5696-2263
Biomedical Engineering, Electrical department, Benha University, Egypt

Therefore, the objectives of this research paper are by providing a new and innovative technique for early detection of stroke, which reduces the risk of death or permanent disability in a non-invasive method by matching electromagnetic waves and finding a relationship between the most important parameters in the study, namely the frequency (F), the electric current (A), the nature of the coil that completes the magnetic field, and the number of turns (N). Different strokes compared to the normal case through the resulting change in the value of the three scenarios that were designed (normal, ischemic, and hemorrhagic) in this way, which can be developed in the future to be a physical device that contributes to the early detection of stroke as much as possible, especially in areas where it is not available expensive techniques, and this will have a great impact in reducing the risk of stroke and its complications.

2. Data and Model

According to what was mentioned in the introduction section of the shortcomings of the currently available techniques for stroke detection, we designed our model that represents blood flow within an artery for three scenarios, the details of which were as graphic (Fig. 1: graphical Artery for the three scenarios: Normal, clotting, and cut positions), Where N for Normal blood flow in one case at scenario 1, and in Ischemic scenario 2 there are 3 positions, D for Down of the artery, M for Middle of the artery and T for the top of the artery. And in Hemorrhagic scenario 3 there are 9 positions, first three positions in Right (R) of the artery, there are D for Down of the artery (RD), C for Center of the artery (RC), and T for the top of the artery (RT). The second three positions in the middle (M) and have also cut at down D to be (MD), Center C (MC), and top T (MT), and the Third three positions in the left (L) side of the artery, down (LD), Center (LC) and top (LT). With a total of 13 models to represent all Scenarios with it is positions.

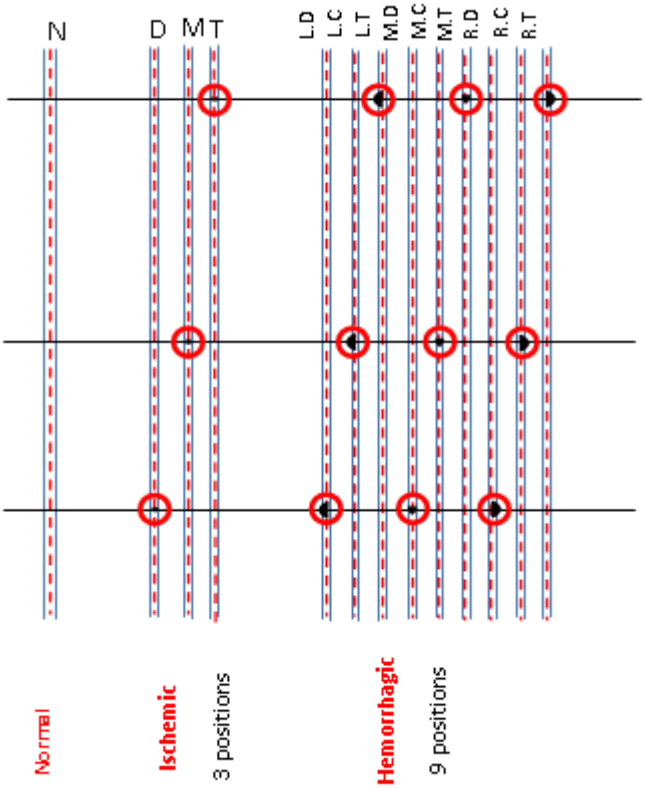

The general design that was built and is the basis for representing all scenarios as shown in (Figure 2: Main Model designed, Laminar flow surrounding by magnetic field) with some minor changes according to each scenario was by our own design and the model was a Cartesian geometry {x, y, z} designed with COMSOL Multi-Physics, and the design center is a cylinder with a liquid with the same density as blood and represents the artery via the Laminar-Flow methodology and surrounded by a coil that represents the Electromagnetic Field, which is a Homogenized multi-turn coil as a conductor model and with a specified number of turns, as detailed later, The coil is Numeric, and coil magnetic vector potential is Quadratic, with current (A) to coil excitation as we need to see the Magnetic Flux Density MFD by applying the electromagnetic wave [15,16], through the blood flowing inside the artery represented by laminar-flow [ref] 17-19 in which the Inlet boundary condition as velocity (u), and the outlet boundary condition as pressure (p). After studying the design used by Muti-Physics for laminar flow and electromagnetic field [Reference] 20-22, then measuring the extent of change in magnetic Flux Density [Reference] 23-26, and according to the design that was created, it shows (Table 1: Model Basic parameters) the most important parameters used in the study of design or model.

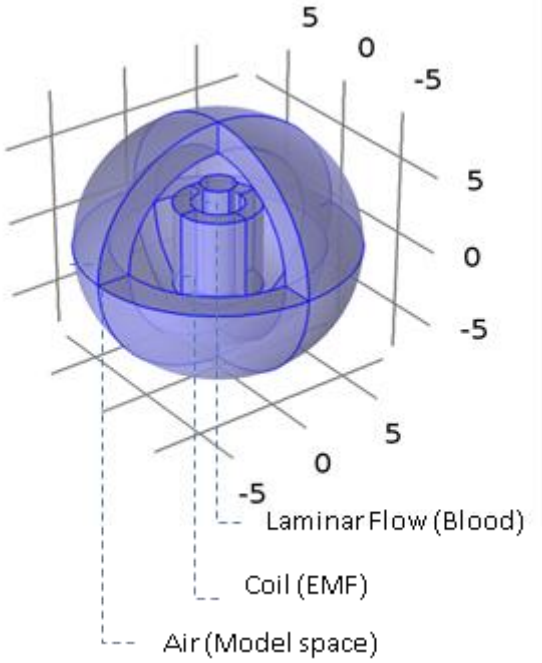

Name	Value	Description	Unit
Frequency -F	(10,15,20)	All	Hz
Relative permeability	1	Air Material parameter	μr
Relative permittivity	1	Air Material parameter	εr
Coil current	(0.5,1,1.5)	Coil-MF	A
Dynamic viscosity	1 Pa·s	Core	μ/mu
Reference temperature	293.15[K] 20 [C]	Laminar Flow	T
Reference pressure level	1[atm]	Laminar Flow	
Blood Density- rho	1060 kg/ m³	Laminar Flow	ρ
Electrical conductivity	0	Air Material parameter	
Number of turns	(20,25)	Coil-MF	n
Coil conductivity	6e7[S/m]	Coil-MF	σ(s/m)
Stabilizatio n	Automatic	Coil-MF	
Relative permeability	1e3	Core	
Electrical conductivity	0	Core	
Relative permittivity	1	Core	
Velocity	u		(m/s)
Pressure/ Absolute pressure	p		(pa)
Electric Field- D	D = ϵ 0 ϵrE		
Magnetic Vector Potential	A		Wb/ m
Magnetic Insulation	= n*A=0		
Coil Length Multiplication factor	1		F_L
Coil Area Multiplication factor	1		F_A
Coil cross-section area	= wire_rad^2*pi		$m2$
Ratio of specific heats	Gamma 1.4		1

3. Methodology

This research presents through our own design-the studying of applying the electromagnetic waves on the blood inside the artery to detect the stroke type in our three scenarios (first scenario: normal blood flow, Second scenario: ischemic that have three positions, and third scenario for hemorrhagic stroke which have nine positions), By Studying the magnetic field, and laminar flow. This study covered three areas. First: coil geometry analysis, Second: stationary, and Third: frequency domain. Regarding to the differentiation in the waves of the Magnetic Flux Density -MFD- norm. The results were promising and distinct for distinguishing between the three scenarios which are normal, ischemic (3 positions), and hemorrhagic (9 positions). And the model block diagram shows the main steps as shown in (fig 3: Model / design

block diagram). In all cases and scenarios, the study was the same to compare the same parameters using the same study depending on the changes at model changed regarding each case/Scenario: the study in normal bold flow, clotting, and cutting scenarios.

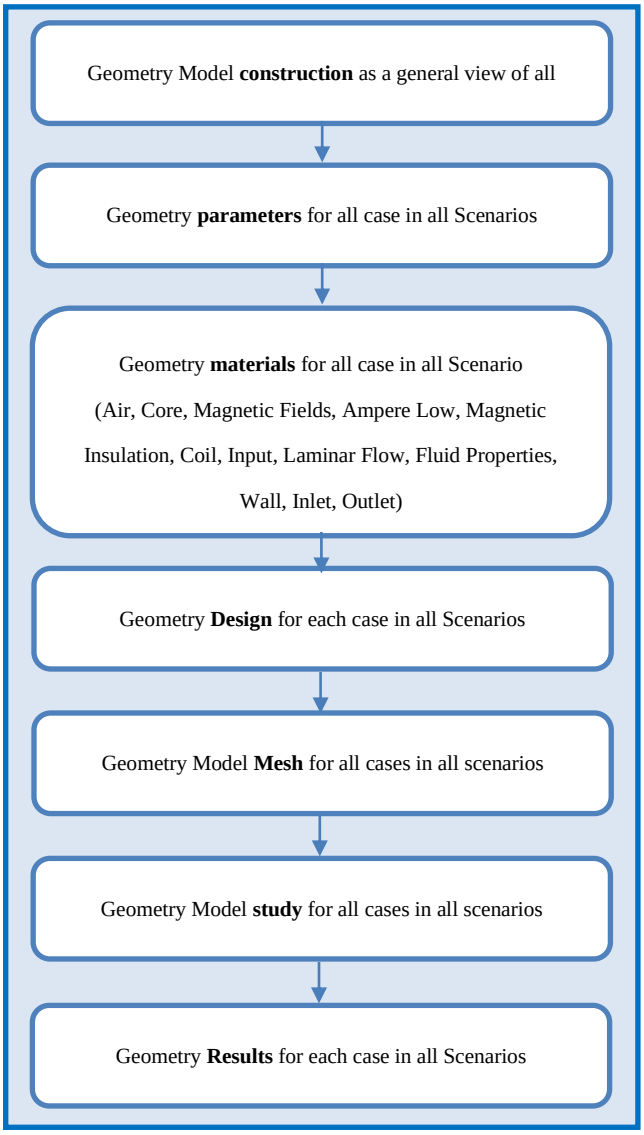

To study the geometries, in all positions, this study goes through the three areas which are. First: The Coil Geometry Analysis, which is used to compute the current flow of a Coil feature in 3D models using the Magnetic Fields interface and the Coil node. The Geometry Analysis sub-node to the Coil feature automatically appears to set up the automatic computation of the current flow in the coil. The boundary conditions for the Geometry Analysis are specified using the Input and Output sub-nodes available with the node. The geometries were analyzed as a physics interface for magnetic fields (mf) and laminar flow (spf) as a Multiphysics [27,28]. Second: Stationary. And it uses a Stationary study type (). For all pure acoustic and vibration problems, this type of analysis yields the zero solution as, by definition, these represent and describe propagating varying fields — either time-dependent or time harmonic in the frequency domain. The geometries were analyzed as a physics interface for magnetic fields (mf) and laminar flow (spf) as a Multiphysics. The stationary solver is used to find the solution to linear and nonlinear stationary problems (also called static or steady-state problems). This solver is automatically used when a Stationary or Frequency Domain study is added to the model [29,32]. And Third: Frequency Domain where wave propagation is modeled by equations from linearized fluid dynamics (pressure waves) and structural dynamics (elastic waves) This procedure is often referred to as working in the frequency domain or Fourier domain as opposed to the time domain. From the mathematical point of view, the time-harmonic equation is a Fourier transform of the original time-dependent equations and its solution as a function of ω is the Fourier transform of a full transient solution. It is therefore possible to synthesize a time-dependent solution from a frequency-domain simulation by applying an inverse Fourier transform [33-35]. The geometries were analyzed as a physics interface for magnetic fields (mf) and laminar flow (spf) as a Multiphysics, using 15 HZ frequency. In all scenarios and cases, Simulation notation of geometry (volume, surfaces, lines, and points) and processed "Entities" Domains, Boundaries, and if applicable edges and points. Common domain was used as mentioned below, with note some changes depending on the different Scenarios and equations is applied in all scenarios as will be explained in detail below.

Model Scenarios

Through the three designed scenario for all cases, normal, Ischemic and hemorrhagic. The Scenario 1 as shown in (fig 4: Model in Normal Scenario) for the normal blood flow, the model features and equations used are: The Magnetic fields (Domains 1–14), Air (Domains 1–7, 9–14), Core (Domain 8), Ampere Low (Domains 1–5, 8–10, 12–13) using the equation (1) $\nabla * H = J$, *where* H *is magnetic field,* J *is current density*. using equation (2) $B = \nabla * A$, *where* B *isutive relation,* A *is coil current*, using equation (3) $J = \sigma E$, *where* σ is coil conductivity.

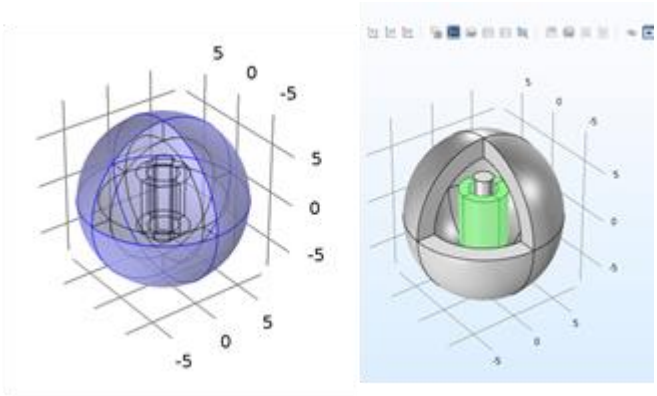

Magnetic Insulation (Boundaries 5–8, 29–30, 41, 46) using equation (4) $n*A=0$, Coil (Domains 6–7, 11, 14) using equation (5) $J\_e=NIcoil/A\ ecoil$, Geometry Analytics (Domains 6–7, 11, 14), Input (Boundary 13) for magnetic field (fig 5: Magnetic Field Input), Laminar Flow (Domain 8) (figure 6: Laminar Flow) using equations (6) $=\nabla.[-\rho I+\mu(\nabla u+(\nabla u)^T)]+F$, $\rho\nabla.(u)=0$, Wall (Boundaries 22–23, 38, 47) using equation U=0, , Inlet (Boundary 24) using equation u=-U0n, Outlet (Boundary 25) using equations (7) $〖[-\rho〗\_I+\mu(\nabla u+(\nabla 〖(u)〗\_^T)]n=-\rho\hat{}0n$, $\rho\hat{}\_0\leq\rho\_0$. With fluid properties equations (8) $=\nabla [-\rho I+\mu(\nabla u+(\nabla u)^T)] +F$, $\rho\nabla (u)=0$

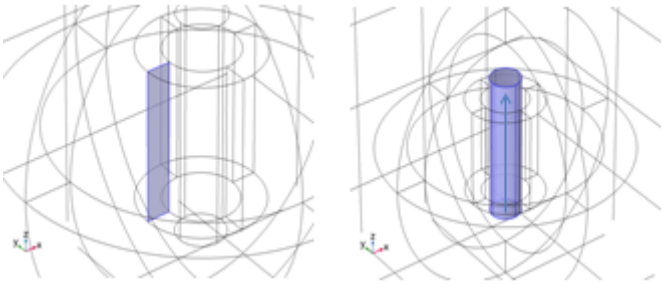

The Scenario 2 as shown in (fig 7: Model in Clotting scenario (Ischemic) position 3- down) For clotting/Ischemic stroke has three positions, Top (T), middle (M) and down (D) of artery designed. Magnetic fields (Domains 1–75), Air (Domain 1–6, 10–42, 44–73, 75), Core (Domains 7–9, 43, 74), Ampere Low (Domains 1–4, 7–41, 43–74) using equations (1) (2), (3), Magnetic Insulation (Boundaries 5–12, 14–25, 107–110, 112–116, 164–165, 168–169, 215, 217–220) using equation (4), Coil (Domains 5–6, 42, 75) using equation (5), Geometry Analytics (Domains 5–6, 42, 75), Input (Boundary 13), Laminar Flow (Domains 7–9, 43, 74) using equation (6), Wall (Boundaries 22–23, 32–33, 35–36, 41, 51–52, 83–84, 93, 99–103, 116, 121, 123, 132, 151, 160–161, 171, 174, 181, 191, 210, 212, 215), Inlet (Boundary 24), Outlet (Boundary 25) using equation (7).

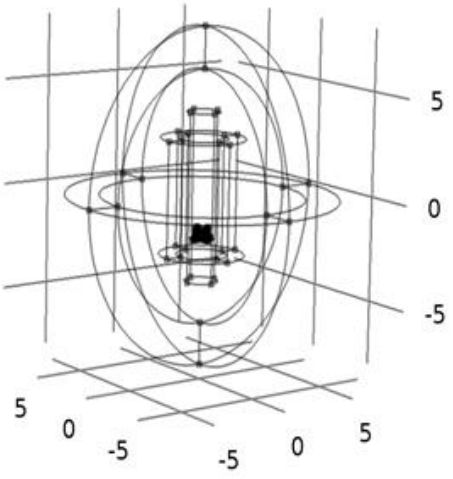

The Scenario 3 as shown in (fig 8: Model in cut scenario (Ischemic) position 1- Top-Right TR)) for cutting/ Hemorrhagic stroke which has nine positions, Magnetic fields (Domains 1–14), Air (Domains 1–7, 9–14), Core (Domain 8), Ampere Low (Domains 1–5, 8–10, 12–13) using equations (1) (2), (3), Magnetic Insulation (Boundaries 5–8, 29–30, 41, 46) using equation (4), Coil (Domains 6–7, 11, 14) using equation (5), Geometry Analytics (Domains 6–7, 11, 14), Input (Boundary 13), Laminar Flow (Domain 8) using equation (6), Wall (Boundaries 22–23, 38, 47, 54–59), Inlet (Boundary 24), Outlet (Boundary 25) using equation (7).

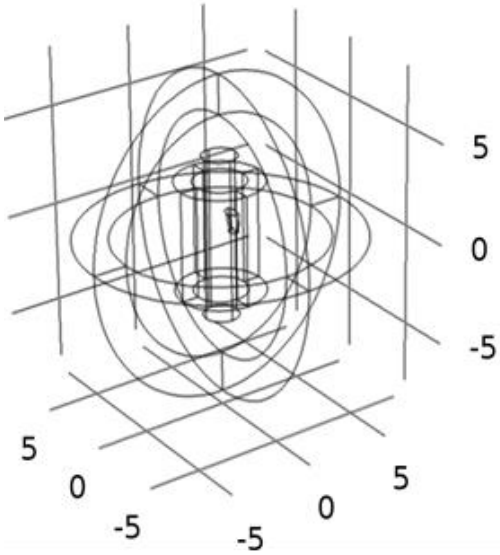

In all three scenarios, the stationary solver 1 with segregated 1 using termination technique with value iterations or tolerance, with the number of iterations 6, it had two segregated steps with linear solver with direct value. The stationary 2 compiled the equations with dependent variables, with 150 as a maximum number of iterations and linear solver value is iterative, in addition, velocity u, pressure ρ. also using direct linear solver with the number of iteration value 2 for auxiliary space Maxwell (AMS) and direct solver value is PARDISO (Parallel Direct Sparse Solver for Clusters). The stationary solver 3 is defined by the study step for frequency domain set at 15 HZ, and fully coupled linear solver with iterative value. In addition, the iterative solver value is BicGStab (biconjugate gradient stabilized iterative method). in this section we have (table 2: MFD norm for three scenarios in all positions designed in our models) which describes the results for all scenarios with it is all positions.

Scenario Number	Name	MFD- Magnetic Flux Density
Scenario 1	Normal blood flow. N	MFD = 0.09 to 3.3*10^-3

Scenario 2	Clotting: [3 positions - Position 1] Middle. M	MFD = 0.08 to 3.15*10^-4
Scenario 2	Clotting: [3 positions - Position 2] Top. T	MFD = 0.08 to 2.99*10^-4
Scenario 2	Clotting: [3 positions - Position 3] Down. D	MFD = 0.08 to 2.99*10^-4
Scenario 3	Cut: [9 positions - Position 1] Right-Center. R. C	MFD = 0.18 to 6.91*10^-3
Scenario 3	Cut: [9 positions - Position 2] Right-Top. R. T	MFD = 0.15 to 5.96*10^-3
Scenario 3	Cut: [9 positions - Position 3] Right-Down. R. D	MFD = 0.17 to 6.69*10^-3
Scenario 3	Cut: [9 positions - Position 4] Left-Top. L.T	MFD = 0.59 to 6.89*10^-3
Scenario 3	Cut: [9 positions - Position 5] Left-Center. L. C	MFD = 0.16 to 5.82*10^-3
Scenario 3	Cut: [9 positions - Position 6] Left-Down. L. D	MFD = 0.15 to 5.56*10^-3
Scenario 3	Cut: [9 positions - Position 7] Middle-Top. M. T	MFD = 0.1 to 4.06*10^-3
Scenario 3	Cut: [9 positions - Position 8] Middle-Center. M.C	MFD = 0.16 to 6.37*10^-3
Scenario 3	Cut: [9 positions - Position 9] Middle-Down. M. D	MFD = 0.15 to 5.82*10^-3

To ensure that our main parameters which are frequency F, Current A, and Coil number of turns N, we tried to fix the current, and change the values for coil turns and frequency, then fixing the frequency and change the current and coil current, and finally, we fixed the coil turns and change the current and the frequency. And this happened in many scenarios, we found that no change in MFD - Magnetic flux density norm results when we change the frequency. at the same time, A and N fixed, (table 3: Results for MFD, F is changing, A and N are fixed 0.5 A, 20 Turns) show some results for a normal Scenario, as the Magnetic flux density norm depends on / is affected by the A and N only.

1. #	**Frequency (F)**	**Current (A)**	**Coil (N)**	**MFD norm**
1	10 Hz	0.5 A	20	0.03 to $1.32*10^{\wedge-3}$
2	15 Hz	0.5 A	20	0.03 to $1.32*10^{\wedge-3}$
3	20 Hz	0.5 A	20	0.03 to $1.32*10^{\wedge-3}$

While fixing the Current A, and increasing the coil turns N, in the same Scenario and frequency is changes, the increase in coil N is affected by 0.3 in MFD norm, (table 4: Results for MFD, F is changing, A and N are fixed 0.5 A, 25 Turns) is showing some results:

1. #	**Frequency (F)**	**Current (A)**	**Coil (N)**	**MFD norm**
4	10 Hz	0.5 A	25	0.04 to $1.65*10^{\wedge-3}$
5	15 Hz	0.5 A	25	0.04 to $1.65*10^{\wedge-3}$
6	20 Hz	0.5 A	25	0.04 to $1.65*10^{\wedge-3}$

In addition, the increasing of current (double 1 A) while frequency is changing and the coil N is fixed as shown in (table 5: Results for MFD, F is changing, A and N are fixed 1 A, 20 Turns), the MFD norm results became two times (double), and the results show that in 0.5 A the MFD value was 0.03 to 1.32*10^-3 and in 1 A the MFD value was 0.07 to 2.46*10^-3.

#	**Frequency (F)**	**Current (A)**	**Coil (N)**	**MFD norm**
7	10 Hz	1 A	20	0.07 to $2.46*10^{\wedge-3}$
8	15 Hz	1 A	20	0.07 to $2.46*10^{\wedge-3}$
9	20 Hz	1 A	20	0.07 to $2.46*10^{\wedge-3}$

And by implementing 1.5 A, as shown in (Table 6: Results for MFD, F is changing, A and N are fixed 1.5 A, 20 & 25

Turns), the MFD norm results became three times when we used 0.5 A and this is mean that the change in frequency did not make any difference, while the increase in coil turns N is affecting the MFD value, also increasing the current A is very effective with N as they are the main effect of MFD norm value. The same tries were run on the other scenarios (clotting & Hemorrhagic), and the analysis of the result is the same.

#	Frequency (F)	Current (A)	Coil (N)	MFD norm
10	10 Hz	1.5 A	20	0.1 to $3.96*10^{-3}$
11	15 Hz	1.5 A	20	0.07 to $2.46*10^{-3}$
12	20 Hz	1.5 A	20	0.07 to $2.46*10^{-3}$
13	10 Hz	1.5 A	25	0.13 to $4.95*10^{-3}$
14	15 Hz	1.5 A	25	0.13 to $4.95*10^{-3}$

4. Results

By observing the results as shown in all designed scenarios, clearly, we can find the differentiation and the changing in the wave and values for the magnetic flux density norm, and among of all parameters which are tested to get the best performance for our simulated work, we find that the best parameters values to study our model using frequency 15 Hz, current 1 A, and the coil with 25 turns. And these parameters values as described in (table 2: MFD norm for three scenarios in all positions designed in our models). The three main scenarios clearly show that the differences of the magnetic flux density norm and this is leads to differentiate fast the normal, Stroke and Hemorrhagic cases, and this is very important to fast and easily predict and differentiate the stroke types which is the main goal for our research.

The results represented in the figure 9: Normal blood flow) for first scenario, then **(**figure 10 a, b, c) for Ischemic or clotting Stroke, and finally the **(**figure 11 a, b, c, d, e, f, g, h, i) for Hemorrhagic or cutting Stroke as discussed in the three cases designed respectively:

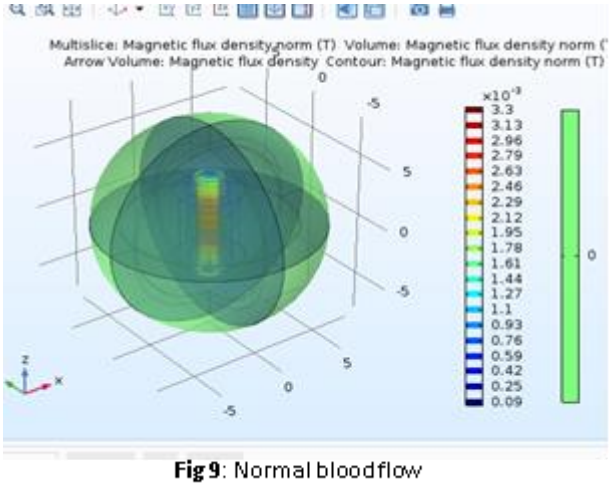

Fig 9: Normal bloodflow

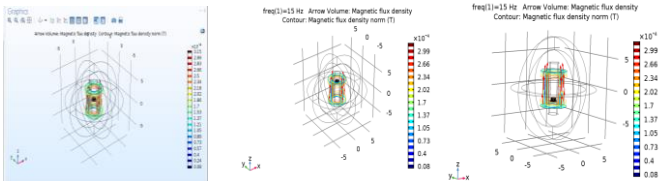

Fig 10 Clotting 3 position: (a) Middle/ (b) above/ (c) Down

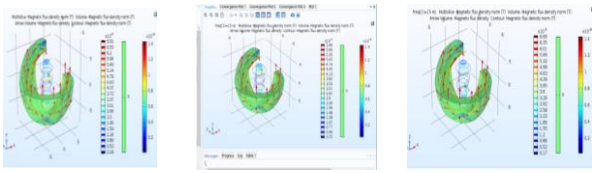

Fig 11 Haemorrhagic 3 positions in Right side of the artery: (a) RC/ (b) RT/ (c) RD

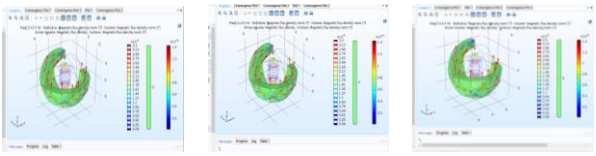

Fig 11 Haemorrhagic 3 positions in Left side of the artery: (d) LT/ (e) LC/ (f) LD

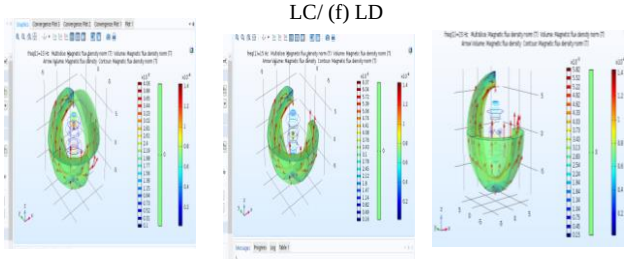

Fig 11 Haemorrhagic 3 positions in Middle of the artery: (g) MT/ (h)

The results above as described to represent it clearly, an average was extracted, where the first case, the value of

magnetic flux density is = 0 in the case of no artery between the two coils, and case 1 the value of magnetic flux density is = from 0.09 to 0.0033 for normal blood flow, then, in case 2 the value of magnetic flux density is = 0.08 to 0.000315 for Ischemic or clotting stroke, and finally case 3 the value of magnetic flux density is = 0.15 to 0.0062 for Hemorrhagic or cutting stroke. the results are represented in (figure 12: Results representation).

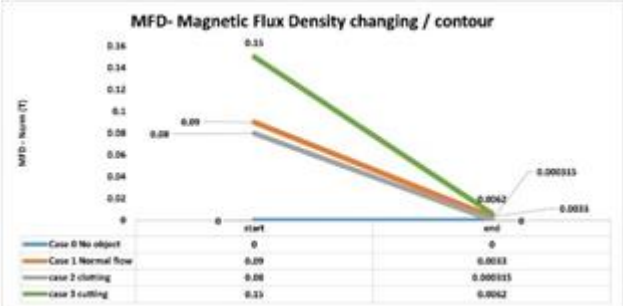

5. Discussion

The cases in all scenarios designed and tested with many varieties to differentiate the stroke types non-invasively, and according to the simulated model designed and represent all possible scenarios for clotting or cutting in the artery, and after changing the basic values of the most influential parameters, we find a clear indicator which approve that every Scenario has a different output in in the magnetic flux density norm or wave depending on the exposure to radiation with low frequency, current. And this is very helpful to quickly know the stroke type and start the first step of medication that can help the patient as it is very important factor as a time to discover because of the late in MRI in different cases, and we have to wait for second scanning after 6 hours minimally, and further to that delay, there is a delay in its treatment according to not discovering immediately, which causes common complications of the disease. The results approve that the Magnetic Flux Density MFD with these criteria studied in our model to be real as a device we can use to predict the Stroke through the excellent features will be used as less time, cheap and safe for all cases in all scenarios.

6. Conclusion

We cannot neglect the current medical devices and it is importance to detect the stroke with each type, but we cannot close our eyes for many cases these devices delayed the prediction of stroke type to detect. In addition, the high cost, for these reasons, we try to find non invasive technique, fast, cheap and safe to predict stroke depending on the change in the waves values represented by own model designed to show this in the magnetic flux density norm values, the clear variances between all scenarios as shown in the results title provided by the research is a very important beginning for the development of the sector of available devices technologies to detect stroke in a simpler, faster, and less expensive way, and this is exactly what we aim to find in near future medically equipped as a device available in all hospitals and examinations center.

7. Future Objectives

The thesis introduced a novel technique to recognize the stroke, and this is the start point in this direction, as a thesis team, we chose to lay a new foundation for a method that will be a cornerstone for much future development and that is through a lot of ideas, among which we can mention, but are not limited to, the following:

- Making more manifold models that simulate exactly the number and locations of arteries within the human brain

- Adding more relationships between arteries in one human brain through more complex designs to reach all scenarios that could be available in any patient.

- The use of the current results and their study with the results of coagulation examinations. Perhaps there is a relationship between the part of the medical analysis and the part of early identification of stroke.

- Develop the practical side software to be a software that works by taking a picture of the head and analyzing it and adding the possibility of artificial intelligence to the subject.

- Developing the project outputs to be more effective and converting them into a device that matches the results of the currently available devices with periodic development to be less expensive, with efficiency close to the available devices, and with faster results.

8. Acknowledgment

This research was partially supported by Faculty of Engineering, Benha University. I thank my professor and academic director Dr. Khaled El-Sayed Ahmed (Khaled S. Ahmed). who provided insight and expertise that greatly assisted the research and his continuous assistance to maximize this research and improved the manuscript.

9. References

[1] E. PMC, “Blunt cerebrovascular injuries: early recognition and stroke prevention in the emergency department.,” Europe PMC. [Online]. Available: https://europepmc.org/article/MED/33320488. [Accessed: 18-Jan-2023].

[2] E. PMC, “Cervical artery dissection: early recognition and stroke prevention.,” Europe PMC, Jul-2016. [Online]. Available:

https://europepmc.org/article/med/27315017. [Accessed: 02-Dec-2020].

[3] B. Dudoignon, L.-E. Tainturier, P. Dodet, G. Bera, E. Groos, C. Chaumereuil, J.-B. Maranci, A. Kas, and I. Arnulf, "Functional brain imaging using 18F-fluorodeoxyglucose positron emission tomography/computerized tomography in 138 patients with Kleine–Levin syndrome: an early marker? ," Academic.oup.com. [Online]. Available: https://academic.oup.com/braincomms/article/3/2/fcab130/6302554?login=true. [Accessed: 18-Jan-2023].

[4] A. Krishna, P. C. Srinivasa Rao, and C. M. A. K. Z. Basha, "Computerized classification of CT lung images using CNN with watershed segmentation," 2020 Second International Conference on Inventive Research in Computing Applications (ICIRCA), Nov. 2020.

[5] Y. Xue, F. G. Farhat, O. Boukrina, A. M. Barrett, J. R. Binder, U. W. Roshan, and W. W. Graves, "A multi-path 2.5 dimensional convolutional neural network system for segmenting stroke lesions in brain MRI images," NeuroImage: Clinical, vol. 25, p. 102118, 2020.

[6] M. D. Rosenberg and H. Song, "Predicting post-stroke aphasia from brain imaging," Nature Human Behaviour, vol. 4, no. 7, pp. 675–676, 2020.

[7] C. Sun, X. Liu, C. Bao, F. Wei, Y. Gong, Y. Li, and J. Liu, "Advanced non-invasive MRI of neuroplasticity in ischemic stroke: Techniques and applications," Life Sciences, vol. 261, p. 118365, 2020.

[8] E. Olgiati and P. A. Malhotra, "Using non-invasive transcranial direct current stimulation for neglect and associated attentional deficits following stroke," Neuropsychological Rehabilitation, vol. 32, no. 5, pp. 735–766, 2020.

[9] M. Pastore-Wapp, T. Nyffeler, T. Nef, S. Bohlhalter, and T. Vanbellingen, "Non-invasive brain stimulation in limb praxis and apraxia: A scoping review in healthy subjects and patients with stroke," Cortex, vol. 138, pp. 152–164, 2021.

[10] L. R. Draaisma, M. J. Wessel, and F. C. Hummel, "Non-invasive brain stimulation to enhance cognitive rehabilitation after stroke," Neuroscience Letters, vol. 719, p. 133678, 2020.

[11] J. Hägglund, "Simulated Cerebrospinal Fluid Motion due to Pulsatile Arterial Flow: Master Thesis Project," DIVA, 29-Apr-2021. [Online]. Available: https://www.diva-portal.org/smash/record.jsf?pid=diva2%3A1546957&dswid=5929. [Accessed: 18-Jan-2022].

[12] Y. Liu, D. Yang, Y. Duo, G. Liu, W. Wang, and B. Xu, "Numerical model and finite element simulation of arterial blood flow profile reconstruction in a uniform magnetic field," Journal of Physics D: Applied Physics, vol. 53, no. 19, p. 195402, 2020.

[13] Y. Wang and W.-N. Lee, "Non-invasive estimation of localized dynamic luminal pressure change by ultrasound elastography in arteries with normal and abnormal geometries," IEEE Transactions on Biomedical Engineering, vol. 68, no. 5, pp. 1627–1637, 2021.

[14] W. Wang, D. Yang, and Y. Lu, "Modeling and simulation of artery occlusion for early detection of carotid atherosclerosis," 2020 Chinese Control And Decision Conference (CCDC), 2020.

[15] A. Farid, A. Najafi, J. Browning, and E. B. Smith, "Electromagnetic waves' effect on airflow during Air Sparging," Journal of Contaminant Hydrology, vol. 220, pp. 49–58, 2019.

[16] "2D simulation of the electromagnetic wave across the non-uniform reentry plasma sheath with Comsol," AIP Advances, vol. 9, no. 5, p. 055316, 2019.

[17] S. S. M and Z. T. Al-sharify, "Simulation of two-phase flow contaminates transport in pipe flow under ...," researchgate, Jun-2020. [Online]. Available: https://www.researchgate.net/publication/343681706_Simulation_of_Two-Phase_Flow_Contaminates_Transport_in_Pipe_Flow_under_Transient_Laminar_Flow_Condition. [Accessed: 18-Jan-2023].

[18] J. Park and Y. S. Song, "Laminar flow manipulators," Extreme Mechanics Letters, vol. 40, p. 100908, 2020.

[19] Z.-H. Han, J. Chen, K.-S. Zhang, Z.-M. Xu, Z. Zhu, and W.-P. Song, "Aerodynamic shape optimization of natural-laminar-flow wing using surrogate-based approach," AIAA Journal, vol. 56, no. 7, pp. 2579–2593, 2018.

[20] L. Aidaoui, Y. Lasbet, and F. Selimefendigil, "Effect of simultaneous application of chaotic laminar flow of nanofluid and non-uniform magnetic field on the entropy generation and energetic/exergetic efficiency," Journal of Thermal Analysis and Calorimetry, vol. 147, no. 10, pp. 5865–5882, 2021.

[21] V. Nabaei, R. Chandrawati, and H. Heidari, "Magnetic biosensors: Modelling and simulation," Biosensors and Bioelectronics, vol. 103, pp. 69–86, 2018.

[22] S. Hariri, M. Mokhtari, M. B. Gerdroodbary, and K. Fallah, "Numerical investigation of the heat transfer of a ferrofluid inside a tube in the presence of

a non-uniform magnetic field," The European Physical Journal Plus, vol. 132, no. 2, 2017.

[23] M. Ulvr, "AC Magnetic Flux Density Standards and their use in Metrology," researchgate, Nov-2020. [Online]. Available: https://www.researchgate.net/profile/Michal-Ulvr/publication/345319602_AC_magnetic_flux_density_standards_and_their_use_in_metrology/links/5fa3b876299bf10f732512a7/AC-magnetic-flux-density-standards-and-their-use-in-metrology.pdf.

[24] R. Blay and R. Porta, "Quick calculation of magnetic flux density in electrical facilities," Applied Sciences, vol. 10, no. 3, p. 891, 2020.

[25] G. Ning, W. Chen, Y. Ling, M. Su, and G. Xu, "Magnetic Flux Density Analysis of series resonant converter operating in discontinuous conduction mode for high-voltage high-power applications," IET Power Electronics, vol. 13, no. 18, pp. 4386–4394, 2020.

[26] F. Chu, Y. Fu, Q. Wang, X. Wu, Z. Liu, and X. Lei, "Analysis of static magnetic flux density and electromagnetic force distribution of a dry-type air-core reactor under different operating current," 2019 22nd International Conference on Electrical Machines and Systems (ICEMS), 2019.

[27] E. H. Flaieh, A. A. Dwech, and M. R. Mosheer, "Modal analysis of fixed - free beam considering different geometric parameters and materials," IOP Conference Series: Materials Science and Engineering, vol. 1094, no. 1, p. 012118, 2021.

[28] L. Qiu, K. Deng, Y. Li, X. Tian, Q. Xiong, P. Chang, P. Su, and L. Huang, "Analysis of coil temperature rise in electromagnetic forming with coupled cooling method," International Journal of Applied Electromagnetics and Mechanics, vol. 63, no. 1, pp. 45–58, 2020.

[29] C. O. M. S. O. L. Multiphysics, "Modeling of charged droplet dynamics in an electric field ... - COMSOL," COMSOL MULTIPHYSICS. [Online]. Available: https://www.comsol.com/paper/download/855251/Sturma_ChargedDroplet-PT_ConfCOMSOL_20.pdf. [Accessed: 18-Jan-2023].

[30] Y. Wang, L.-M. He, Z. Li, W. Xu, and J. Ren, "A computationally efficient nonlinear dynamic model for CMUT based on Comsol and MATLAB/simulink," 2020 IEEE 15th International Conference on Solid-State & Integrated Circuit Technology (ICSICT), 2020.

[31] A. Seguin, Y. Bertho, F. Martinez, J. Crassous, and P. Gondret, "Experimental velocity fields and forces for a cylinder penetrating into a granular medium," Physical Review E, 10-Jan-2013. [Online]. Available: https://link.aps.org/doi/10.1103/PhysRevE.87.012201. [Accessed: 18-Jan-2023].

[32] S. E. Savotchenko, "Stationary states near the interface with anharmonic properties between linear and nonlinear Defocusing Media," Solid State Communications, vol. 283, pp. 1–8, 2018.

[33] A. V. Syutkin, G. A. Evdokunin, and I. V. Popov, "Methodology of determining frequency response of grounding systems using the COMSOL Multiphysics Software," 2021 IEEE Conference of Russian Young Researchers in Electrical and Electronic Engineering (ElConRus), 2021.

[34] Z.-X. Du, A. Li, X. Y. Zhang, and D. F. Sievenpiper, "A simulation technique for radiation properties of time-varying media based on frequency-domain solvers," IEEE Access, vol. 7, pp. 112375–112383, 2019.

[35] P. Bekemeyer, R. Thormann, and S. Timme, "Frequency-domain gust response simulation using computational fluid dynamics," AIAA Journal, vol. 55, no. 7, pp. 2174–2185, 2017.